



**HAL**  
open science

# The role of aromatic precursors in the formation of haloacetamides by chloramination of dissolved organic matter

Julien Le Roux, Maolida Nihemaiti, Jean-Philippe Croué

► **To cite this version:**

Julien Le Roux, Maolida Nihemaiti, Jean-Philippe Croué. The role of aromatic precursors in the formation of haloacetamides by chloramination of dissolved organic matter. *Water Research*, 2016, 88, pp.371-379. 10.1016/j.watres.2015.10.036 . hal-01305549

**HAL Id: hal-01305549**

**<https://enpc.hal.science/hal-01305549>**

Submitted on 30 Apr 2016

**HAL** is a multi-disciplinary open access archive for the deposit and dissemination of scientific research documents, whether they are published or not. The documents may come from teaching and research institutions in France or abroad, or from public or private research centers.

L'archive ouverte pluridisciplinaire **HAL**, est destinée au dépôt et à la diffusion de documents scientifiques de niveau recherche, publiés ou non, émanant des établissements d'enseignement et de recherche français ou étrangers, des laboratoires publics ou privés.

Copyright

# The role of aromatic precursors in the formation of haloacetamides by chloramination of dissolved organic matter

*Julien Le Roux<sup>a,b</sup>, Maolida Nihemaiti<sup>a,c</sup>, Jean-Philippe Croué<sup>a,c,\*</sup>*

<sup>a</sup> Water Desalination and Reuse Center, 4700 KAUST, Thuwal 23955-6900, Saudi Arabia

<sup>b</sup> LEESU (UMR MA 102), Université Paris-Est - AgroParisTech, 61 avenue du Général de Gaulle, 94010 Créteil cedex, France

<sup>c</sup> Curtin Water Quality Research Centre, Department of Chemistry, Curtin University, GPO Box U1987, Perth WA 6845

\* Corresponding author

E-mail addresses: [julien.le-roux@u-pec.fr](mailto:julien.le-roux@u-pec.fr) (J. Le Roux), [maolida.nihemaiti@kaust.edu.sa](mailto:maolida.nihemaiti@kaust.edu.sa) (M. Nihemaiti), [jean-philippe.croue@curtin.edu.au](mailto:jean-philippe.croue@curtin.edu.au) (Jean-Philippe Croué)

## **Abstract**

Water treatment utilities are diversifying their water sources and often rely on waters enriched in nitrogen-containing compounds (e.g., ammonia, organic nitrogen such as amino acids). The disinfection of waters exhibiting high levels of nitrogen has been associated with the formation of nitrogenous disinfection byproducts (N-DBPs) such as haloacetonitriles (HANs) and haloacetamides (HAcAms). While the potential precursors of HANs have been extensively studied, only few investigations are available regarding the nature of HAcAm precursors. Previous research has suggested that HAcAms are hydrolysis products of HANs. Nevertheless, it has been recently suggested that HAcAms can be formed independently, especially during chloramination of humic

25 substances. When used as a disinfectant, monochloramine can also be a source of nitrogen for  
26 N-DBPs. This study investigated the role of aromatic organic matter in the formation of N-DBPs  
27 (HAcAms and HANs) upon chloramination. Formation kinetics were performed from various  
28 fractions of organic matter isolated from surface waters or treated wastewater effluents.  
29 Experiments were conducted with  $^{15}\text{N}$ -labeled monochloramine ( $^{15}\text{NH}_2\text{Cl}$ ) to trace the origin of  
30 nitrogen. N-DBP formation showed a two-step profile: (1) a rapid formation following second-order  
31 reaction kinetics and incorporating nitrogen atom originating from the organic matrix (e.g., amine  
32 groups); and (2) a slower and linear increase correlated with exposure to chloramines, incorporating  
33 inorganic nitrogen ( $^{15}\text{N}$ ) from  $^{15}\text{NH}_2\text{Cl}$  into aromatic moieties. Organic matter isolates showing high  
34 aromatic character (i.e., high SUVA) exhibited high reactivity characterized by a major  
35 incorporation of  $^{15}\text{N}$  in N-DBPs. A significantly lower incorporation was observed for low-  
36 aromatic-content organic matter.  $^{15}\text{N}$ -DCAcAm and  $^{15}\text{N}$ -DCAN formations exhibited a linear  
37 correlation, suggesting a similar behavior of  $^{15}\text{N}$  incorporation as SUVA increases. Chloramination  
38 of aromatic model compounds (i.e., phenol and resorcinol) showed higher HAcAm and HAN  
39 formation potentials than nitrogenous precursors (i.e., amino acids) usually considered as main  
40 precursors of these N-DBPs. These results demonstrate the importance of aromatic organic  
41 compounds in the formation of N-DBPs, which is of significant importance for water treatment  
42 facilities using chloramines as final disinfectant.

43

44

#### 45 **Keywords**

46 Chloramination, disinfection byproducts, haloacetamides, dissolved organic matter, aromatic  
47 compounds

48

49

50

51

52

### 53 **1. Introduction**

54 Surface waters are often impacted by human activities (e.g., agriculture, industries, and municipal  
55 wastewater effluent discharges) resulting in their enrichment in nitrogen-containing compounds  
56 (i.e., ammonia and organic nitrogen such as amino acids) (Westerhoff and Mash, 2002). The  
57 disinfection of waters exhibiting high levels of nitrogen has been associated with the formation of  
58 nitrogenous disinfection byproducts (N-DBPs) (Bond et al., 2011). N-DBPs generally form in  
59 significantly lower concentrations than regulated DBPs, but have been a growing concern over the  
60 past decade because of their higher health risk (Muellner et al., 2007; Plewa et al., 2004). *In vitro*  
61 mammalian cell tests have demonstrated that haloacetonitriles (HANs), halonitromethanes (HNMs),  
62 and haloacetamides (HAcAms) are more cytotoxic and genotoxic (i.e., up to 2 orders of magnitude)  
63 than non-nitrogenous molecules such as trihalomethanes (THMs) and haloacetic acids (HAAs)  
64 (Plewa et al., 2008). Nitrogen in N-DBPs can also be derived from chloramines when used as  
65 disinfectants. Water utilities have been increasingly switching to monochloramine as an alternative  
66 to chlorine in order to limit the production of regulated THMs and HAAs. Nevertheless, concern  
67 has been raised regarding the formation of N-DBPs (e.g., N-nitrosodimethylamine - NDMA)  
68 produced from the reaction between monochloramine and secondary or tertiary amines (Mitch and  
69 Sedlak, 2004).

70 Among N-DBPs, dichloroacetonitrile (DCAN) and dichloroacetamide (DCAcAm) are the most  
71 frequently detected species in drinking water treatment plants (Krasner et al., 2006). While the  
72 potential precursors of HANs have been extensively studied, only few investigations are available  
73 regarding the nature of HAcAms precursors. HAcAms were first reported to be intermediate  
74 products of HANs hydrolysis and ultimately decomposed to HAAs (Glezer et al. 1999, Reckhow et  
75 al. 2001). More recently, it was found that HAcAms can be formed independently from HANs  
76 during chlorination and chloramination processes (Huang et al., 2012). Two different pathways have

77 been proposed to describe the formation of HANs and HAcAms (Fig. S1). First, the  
78 Decarboxylation Pathway occurs by rapid chlorination or chloramination of  $\alpha$ -amine groups of free  
79 amino acids to form a nitrile, followed by hydrolysis to release HANs and carbonic acid (Trehy et  
80 al., 1986). HANs are then further hydrolyzed to HAcAms and HAAs (Reckhow et al., 2001). The  
81 second pathway proposed for HANs formation is the Aldehyde Pathway, where nitrogen from  
82 monochloramine ( $\text{NH}_2\text{Cl}$ ) is incorporated into aldehydes to produce nitriles. The reaction between  
83  $\text{NH}_2\text{Cl}$  and formaldehyde forms cyanogen chloride ( $\text{CNCl}$ ) (Pedersen et al., 1999), and  
84 chloroacetonitrile is formed from chloroacetaldehyde (Kimura et al., 2013). Haloacetaldehydes  
85 (HAcAls) are carbonaceous DBPs frequently detected in disinfected waters, and often represent the  
86 third major class of DBPs after THMs and HAAs (Krasner et al., 2006). Chloroacetaldehyde has  
87 been demonstrated to be a precursor of N,2-dichloroacetamide upon chloramination (Kimura et al.,  
88 2013). The reaction involves the incorporation of the nitrogen atom of monochloramine ( $\text{NH}_2\text{Cl}$ ) to  
89 form the amide group through the formation of a carbinolamine intermediate.

90 In addition to the Aldehyde Pathway, most studies about HANs and HAcAms formation  
91 mechanisms focused on the chlorination of nitrogenous precursors (e.g., amino acids, amines,  
92 pyrimidines) or matrices enriched in nitrogenous moieties (e.g., algae cells, extracellular organic  
93 matter) (Bond et al., 2009; Fang et al., 2010; Oliver, 1983; Reckhow et al., 2001; Yang et al., 2010,  
94 2011, 2012). In the case of aquatic humic substances, a positive correlation was found between their  
95 nitrogen content and their tendency to form HAN upon chlorination (Reckhow et al., 1990). Studies  
96 performed with labeled  $^{15}\text{N}$ -chloramines ( $^{15}\text{NH}_2\text{Cl}$ ) on nitrogenous organic (N-org) precursors and  
97 fractions of dissolved organic matter (DOM) found that nitrogen in HANs or  $\text{CNCl}$  originated from  
98 both organic precursors and  $\text{NH}_2\text{Cl}$  (Yang et al., 2010). Recent studies suggested that aromatic  
99 moieties of DOM may contribute to a substantial HAN formation upon chloramination (Chuang et  
100 al., 2013; Huang et al., 2012; Yang et al., 2008, 2010). During chloramination, the formation of  
101 DCAN or  $\text{CNCl}$  did not correlate with the DON/DOC ratios of DOM fractions. However, good  
102 correlations were observed with their SUVA values and thus with their aromatic carbon content

103 (Yang et al., 2008). A mechanism describing the chloramination of a  $\beta$ -diketone moiety was  
104 proposed based on the Decarboxylation Pathway, showing the incorporation of nitrogen through the  
105 formation of an *N*-chloroimine and leading to DCAN as a hydrolysis product. Approximately 90 %  
106 of nitrogen in DCAN and CNCl was reported to originate from  $\text{NH}_2\text{Cl}$  reaction with Suwannee  
107 River DOM (Yang et al., 2010). Recent kinetics experiments also suggest similarities between  
108 HANs, THMs, and HAAs precursors (Chuang et al., 2013). Kinetics of DCAN and  
109 trichloronitromethane (TCNM) formation upon chloramination using  $^{15}\text{NH}_2\text{Cl}$  were proposed to  
110 involve two reaction mechanisms: formation from N-org precursors following a second-order  
111 reaction; and formation by incorporation of nitrogen from  $\text{NH}_2\text{Cl}$ , linearly correlated with  
112 chloramines exposure (Chuang and Tung, 2015).

113 Less information is available about HAcAms precursors and formation mechanisms, since HAcAms  
114 were first reported as DBPs in a 2000-2002 drinking water survey (Krasner et al., 2006; Weinberg et  
115 al., 2002). Although DCACAm yields from amino acids are considerably lower than those of  
116 DCAN, comparable levels (i.e., median concentrations of 1.3 and 1  $\mu\text{g/L}$ , respectively) have been  
117 observed in US drinking waters (Bond et al., 2012; Krasner et al., 2006). Therefore, unknown  
118 precursors appear to be responsible for the majority of HAcAm formation (Bond et al., 2012). The  
119 formation of HAcAms from algal exopolymeric substances (EPS), municipal wastewater treatment  
120 plant effluents (Huang et al., 2012), natural waters (Chu et al., 2013), bacterial cells (Huang et al.,  
121 2013), natural organic matter (NOM) fractions, and free amino acids (Chu et al., 2010a, 2010b) has  
122 been previously studied. The hydrophilic acid fraction isolated from an algal-impacted water  
123 enriched in nitrogen (i.e., high DON/DOC ratio), exhibited the highest DCACAm formation  
124 potential during both chlorination and chloramination, which was associated with the presence of  
125 protein-like organic matter (Chu et al., 2010b). However, DCACAm was recently found to be  
126 preferentially formed by chloramination of humic materials, while chlorination of wastewater  
127 effluents and algal EPS tended to form more DCAN (Huang et al., 2012). These results suggested  
128 that the mechanism of HAcAms formation is independent from that of HANs. Overall, HAcAms

129 formation mechanisms remain unclear, and the precursors of HAcAms in natural waters still need to  
130 be characterized.

131 This study investigated the role of aromatic organic matter in the formation of N-DBPs (i.e.,  
132 especially HAcAms) upon chloramination, with emphasis on the formation kinetics of HAcAms  
133 and HANs. Various fractions of organic matter isolated from different waters (i.e., surface waters,  
134 treated wastewater) as well as model compounds were studied to understand the factors controlling  
135 N-DBPs formation. Experiments were conducted with  $^{15}\text{NH}_2\text{Cl}$  to trace the origin of nitrogen in the  
136 formed DBPs.

137

## 138 **2. Materials and methods**

### 139 **2.1. Materials**

140 All reagents were of analytical or laboratory grade and were used without further purification.  
141 MilliQ water was produced with a Millipore system (18.2 M $\Omega$ .cm). Sodium hypochlorite (NaOCl,  
142 5.65-6%, Fisher Scientific) and ammonium chloride (Acros Organics, 99.6%) were used to prepare  
143 chloramine reagents.  $^{15}\text{N}$ -labeled ammonium chloride was purchased from Sigma-Aldrich (98%).  
144 Sodium thiosulfate (Fisher Scientific) was used to quench residual chloramines. Methyl tert-butyl  
145 ether (MTBE) and ethyl acetate (> 99%, Fisher Scientific) were used for DBP extractions without  
146 further purification. A THM calibration mix (chloroform - TCM, dichlorobromomethane -  
147  $\text{CHCl}_2\text{Br}$ , chlorodibromomethane -  $\text{CHClBr}_2$ , and bromoform - TBM), a mixed standard (EPA 551B  
148 Halogenated Volatiles Mix) containing haloacetonitriles (HANs), trichloronitromethane (TCNM, or  
149 chloropicrin) and haloketones (HKs), and a mixed standard containing 9 HAAs (EPA 552.2 Methyl  
150 Ester Calibration Mix) were supplied from Supelco (Sigma-Aldrich). Chloro-, bromo-, dichloro-,  
151 and trichloroacetamide were obtained from Sigma-Aldrich. Other haloacetamides (HAcAms) were  
152 purchased from Cansyn Chem. Corp. Decafluorobiphenyl (99%, Sigma-Aldrich, Supelco) was used  
153 as a surrogate standard. 2-bromopropionic acid (Fluka Analytical) was used as a surrogate for HAA  
154 extractions and analyses. Phenol (>99%), resorcinol (>99%), L-tyrosine (>98%), L-aspartic acid

155 (>99.5%) and L-tryptophan (>98%) were obtained from Sigma-Aldrich.

## 156 **2.2. Experimental methods**

157 All glassware used during these experiments was washed with Milli-Q water and baked at 500°C  
158 for at least 5 h prior to use. DOM stock solutions were prepared by dissolving 20 mg of a selected  
159 DOM isolate in 500 mL of Milli-Q water (dissolved organic carbon, i.e., DOC ~ 14-19 mg C/L).  
160 Solutions for experimentation were prepared by adjusting DOC to 5 mg C/L in 10 mM phosphate  
161 buffer. Monochloramine and <sup>15</sup>N-labeled monochloramine stock solutions were prepared by adding  
162 sodium hypochlorite (NaOCl) to a continuously-stirred ammonium chloride or <sup>15</sup>N-labeled  
163 ammonium chloride solution, respectively, adjusted to pH 8.5 with sodium hydroxide, at a N:Cl  
164 molar ratio of 1.2:1. The concentration of monochloramine stock solutions was adjusted to a desired  
165 concentration. Chloramination experiments were performed in headspace-free 65 mL amber glass  
166 bottles under excess of disinfectant dosage. The doses were calculated as:  $\text{NH}_2\text{Cl (mg/L as Cl}_2) = 3$   
167  $\times \text{DOC (mg C/L)}$ , to conduct a comprehensive comparison between our DBPFP data and results  
168 obtained from other studies working with similar doses (Chu et al., 2010b; Dotson et al., 2009;  
169 Krasner et al., 2007). Monochloramine was also added in excess for the determination of DBPFP of  
170 model organic compounds (i.e., phenol, resorcinol, tyrosine, aspartic acid, and tryptophan) solutions  
171 (chloramine/model compound molar ratio = 5.6). Most of the experiments were conducted in  
172 duplicates, at room temperature (22±1°C), and under dark conditions to avoid any photolysis  
173 reaction. At the end of the reaction time, chlorine residual was quenched using a slight excess of  
174 sodium thiosulfate. To avoid any loss of the targeted by-products, samples were extracted  
175 immediately after quenching. Free chlorine and total chlorine concentrations in the stock solutions  
176 of sodium hypochlorite were determined iodometrically with sodium thiosulfate 0.1 M (>99.9%).  
177 Initial  $\text{NH}_2\text{Cl}$  and  $\text{NHCl}_2$  concentrations were determined by spectrophotometric measurement  
178 using their respective molar extinction coefficients at 245 nm and 295 nm and by solving  
179 simultaneous equations (Schreiber and Mitch, 2005). Residual oxidant was analyzed iodometrically  
180 (Eaton et al., 1995). Oxidant exposures were calculated based upon the integration of concentration

181 versus time curves of oxidant decay.

### 182 **2.3. Analytical methods**

183 Total Organic Carbon (TOC) and Total Nitrogen (TN) concentrations were measured using a TOC  
184 analyzer equipped with a TN detection unit (TOC-VCSH, Shimadzu). UV<sub>254</sub> absorbance was  
185 measured using UV-Vis spectrometer (UV-2550, Shimadzu) and specific UV absorbance at 254 nm  
186 (SUVA) values were calculated as UV<sub>254</sub>/DOC ratio and expressed as L.mg<sup>-1</sup>.m<sup>-1</sup>. Four  
187 trihalomethanes (THMs), four haloacetonitriles (HANs), two haloketones (HKs), and chloropicrin  
188 were extracted and analyzed following EPA method 551, which consists of a liquid-liquid extraction  
189 using MTBE followed by gas chromatography coupled with electron capture detector (GC-ECD) or  
190 mass spectrometer (GC-MS) (Munch and Hautman, 1995). Nine HAAs were extracted and  
191 analyzed following EPA method 552.2, which is based on a liquid-liquid extraction with MTBE in  
192 acidic conditions followed by derivatization to methyl esters using acidic methanol, and analysis by  
193 gas chromatography coupled with mass spectrometry (GC-MS) (Munch and Munch, 1995).  
194 HAcAms were analyzed following the same EPA method 551 protocol, replacing MTBE by ethyl  
195 acetate for the liquid-liquid extraction. For experiments involving <sup>15</sup>N-NH<sub>2</sub>Cl, all extracts were  
196 analyzed by GC-MS. Since <sup>15</sup>N-labeled DBPs (<sup>15</sup>N-DBPs) are not commercially available, the  
197 concentration of <sup>15</sup>N-DBPs was quantified indirectly using the concentration of unlabeled DBPs  
198 (i.e., <sup>14</sup>N-DBPs), based on the assumption that the MS response for <sup>14</sup>N-DBPs is similar to that for  
199 <sup>15</sup>N-DBPs (Huang et al., 2012). As an example, DCAN concentrations were determined using m/z  
200 74 and 75 as quantification ions for <sup>14</sup>N-DCAN and <sup>15</sup>N-DCAN, respectively, and using the  
201 calibration curve obtained from <sup>14</sup>N-DCAN standards. The same method was used for other  
202 <sup>15</sup>N-DBPs analysis. Additional analytical details and the list of labeled and unlabeled DBPs and  
203 their related quantification ions are provided in [Text S1](#) and [Table S1](#) (SI).

### 204 **2.4. Characteristics of DOM extracts**

205 Samples of wastewater were collected at the Jeddah wastewater (JW) treatment plant (Saudi Arabia)  
206 in September 2012 and stored at 4°C prior to the extraction. The hydrophobic (JW HPO),

207 transphilic (JW TPI), and colloidal (JW COL) effluent organic matter (EfOM) fractions were  
208 obtained from these samples. Three previously isolated hydrophobic NOM fractions (i.e.,  
209 hydrophobic acids-HPOA obtained from base desorption, and hydrophobic-HPO isolated with  
210 acetonitrile/water desorption) showing different chemical composition were selected: SR HPOA  
211 isolated from the Suwannee River (Georgia, USA), BR HPO isolated from the Blavet River (Côte  
212 d'Armor, France), and GR HPO obtained from the Gartempe River (Vienne, France). One  
213 hydrophilic acid (RR HPI) isolated from the Ribou River (Maine-et-Loire, France) was also  
214 selected. NOM fractions were isolated using two slightly different comprehensive isolation  
215 protocols described elsewhere (Croué, 2004; Leenheer et al., 2000). All fractions and their chemical  
216 compositions are described in [Table S2](#) (SI).

217

### 218 **3. Results and discussion**

#### 219 **3.1. Kinetics of DBP formation**

220 In preliminary experiments, the kinetics of DBPs formation were assessed during chloramination  
221 over 72h on EfOM isolates (JW HPO and JW TPI) and Suwannee River NOM (SR HPOA).

222 Monochloramine concentration remained in excess during all the reaction time ([Fig. S2](#), SI). The  
223 decay of monochloramine was always caused by its autodecomposition since no significant  
224 variations were observed between all the experiments, and the experimental values fitted well with  
225 the autodecomposition model reported by Jafvert and Valentine (1992).

226 DCACAm formation from the three isolates (SR HPOA, JW HPO, JW TPI) showed a two steps  
227 profile: a rapid formation in the first 3 hours of reaction, followed by a linear increase ([Fig. 1a](#)). The  
228 formation of DCACAm from JW TPI increased slightly faster than from JW HPO during the first 24  
229 hours of reaction, and then slowed down between 24h and 72h. A linear increase was observed for  
230 JW HPO, finally reaching a concentration similar to that of JW TPI at 72h of reaction (42.9 nM and  
231 38.6 nM for JW HPO and JW TPI, respectively). This finding indicates that the nature of EfOM  
232 precursors (as described by their C/N ratio and hydrophobicity in terms of SUVA values, see [Table](#)

233 [S2](#), SI) might play an important role in formation kinetics, but exerts a lesser influence on the  
234 overall formation potential. A lower concentration of nitrogenous precursors in JW HPO (i.e., as  
235 revealed by its higher C/N ratio of 19.5, compared to 8.4 for JW TPI, [Table S2](#), SI) could lead to a  
236 lower formation of DCaAm in the first 24 hours of reaction, then slow incorporation of nitrogen  
237 from monochloramine into the organic matrix would occur with time, leading to a continuous  
238 increase in DCaAm. DCaAm formation kinetics from SR HPOA was significantly faster than  
239 that from EfOM isolates. DCaAm concentration quickly increased in the first 10 hours of reaction,  
240 and then linearly increased even faster after 10h to reach a final concentration of 169.2 nM (21.7  
241 µg/L) at 48h. The high reactivity of SR HPOA isolate can be related to its aromatic character (i.e.,  
242 SUVA value = 4.6). High SUVA NOM isolates are generally characterized by a low incorporation of  
243 nitrogenous moieties, i.e., high C/N ratio (e.g., C/N ratio of 68.6 for SR HPOA) as compared to  
244 other isolates ([Table S2](#), SI) (Leenheer and Croué, 2003). In addition, the substantial difference  
245 between SR HPOA and JW HPO reactivities can be explained by their different origins. Especially,  
246 EfOM and NOM exhibit different relationships between SUVA and the aromatic carbon content,  
247 which is explained by a different origin of aromatic moieties (Drewes and Croué, 2002).  
248 Furthermore, EfOM contains less high molecular weight compounds, less compounds with CHO  
249 formulae but much more organosulfur compounds with CHOS formulae (e.g., surfactants) as  
250 compared to NOM (Gonsior et al., 2011).  
251 DCaAm concentrations from the three isolates did not stabilize after 72h, thus indicating that  
252 precursors were still available in the solutions. No TCaAm was detected (detection limit of 4 nM)  
253 from any isolate in the experimental conditions used (i.e.,  $\text{NH}_2\text{Cl} = 15 \text{ mg Cl}_2/\text{L}$  and Cl:N ratio of  
254 1:1.2). No brominated HAcAms were detected since no bromide was present in the reaction  
255 solutions.  
256 DCAN formation from the three isolates followed similar profiles compared to those of DCaAm  
257 formation ([Fig. 1b](#)). The difference between JW HPO and JW TPI isolates was even more  
258 pronounced: a faster reactivity was observed for JW TPI between 0 and 24 hours of reaction, but it

259 slowed down to reach a final concentration of 23.1 nM after 72h. JW HPO profile showed a  
 260 progressive increase with time, to finally reach a higher concentration (i.e., 30.3 nM) than that of  
 261 JW TPI. As discussed for DCACAm results, the different nature of DBP precursors present in the  
 262 two JW EfOM isolates (i.e., different proportion of aromatic and nitrogenous precursors), may  
 263 influence the reaction kinetics. DCAN formation from SR HPOA was also considerably more  
 264 important than from JW EfOM isolates and increased faster, reaching 92.5 nM after only 48h. No  
 265 other HAN was detected from any of the three isolates.

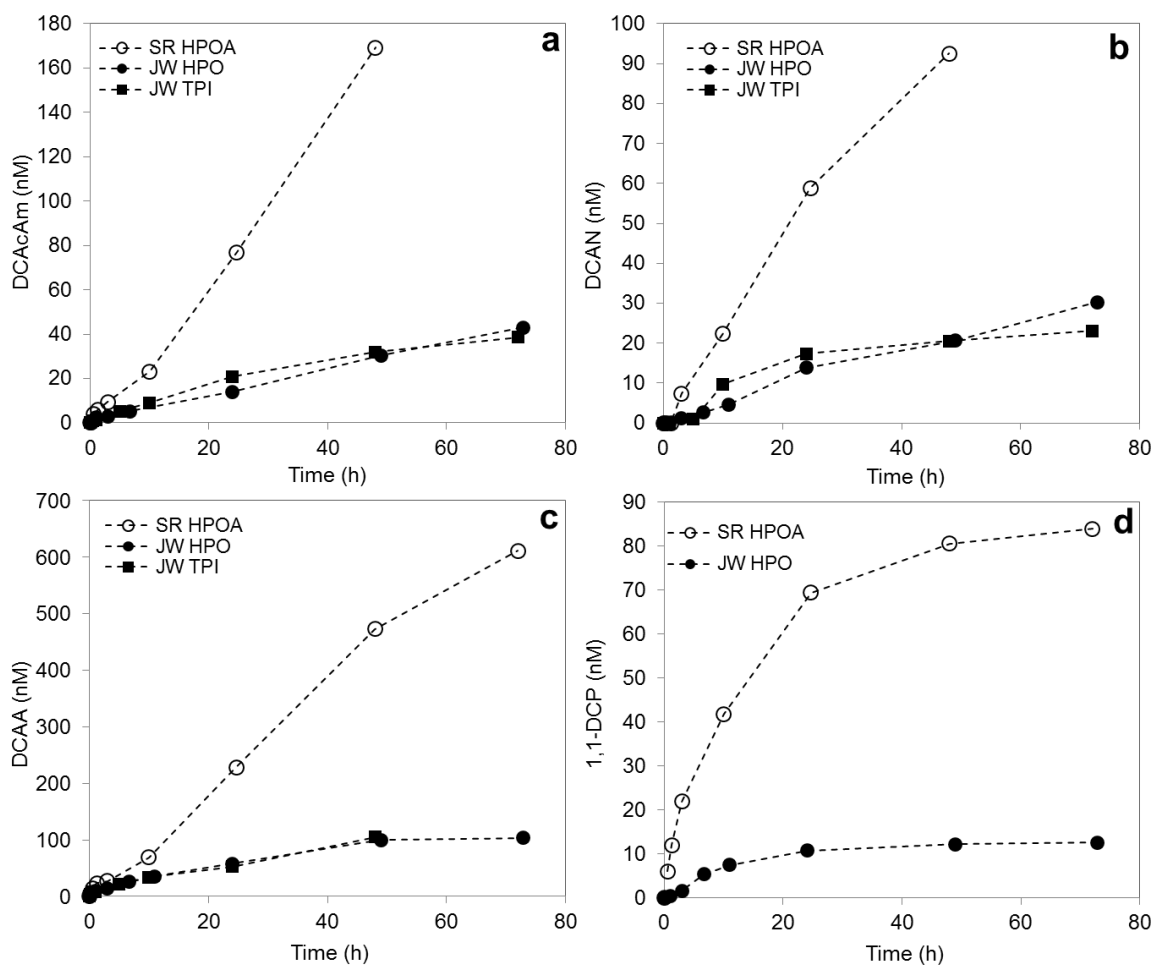


Figure 1. Formation kinetics of a) DCAcAm, b) DCAN, c) DCAA, and d) 1,1-DCP by chloramination (15 mg Cl<sub>2</sub>/L) of SR HPOA, JW HPO, and JW TPI isolates (5 mg C/L) at pH 8 (10 mM phosphate buffer).

266 DCAA was the major DBP detected during these experiments, with concentrations of 611.0 nM and  
 267 103.1 nM formed after 72h for SR HPOA and JW HPO, respectively. The SR HPOA isolate was the

268 strongest DCAA precursor with a kinetics profile similar to that of DCACAm. A similar DCAA  
269 formation was observed for the two JW EfOM isolates indicating that, unlike N-DBPs, DCAA  
270 precursors might be more similar in the two fractions. TCAA was only detected at very low  
271 concentrations ( $< 0.005$  nM, i.e.,  $< 0.8$   $\mu\text{g/L}$ ) for SR HPOA and JW TPI.  
272 TCM was only detected for SRHPOA, reaching a concentration of 453.1 nM after 72h.  
273 1,1-dichloropropanone (1,1-DCP) was solely detected during the chloramination of SR HPOA and  
274 JW HPO. This observation could be related to the higher proportion of aromatic precursors in these  
275 isolates. The formation of HKs has been previously reported from chlorination and chloramination  
276 of Black Lake fulvic acids and a Suwannee River reverse osmosis NOM isolate (Reckhow and  
277 Singer, 1985; Yang et al., 2007). 1,1-DCP formation rates from both isolates quickly increased in  
278 the first 24 hours of reaction, but decreased after 24h to reach final concentrations (at 72h) of 84.0  
279 nM and 12.6 nM for SR HPOA and JW HPO, respectively. HKs are known as intermediates in the  
280 haloform reaction, hydrolyzing to chloroform in neutral and alkaline conditions (Suffet et al., 1976).  
281 The formation of HKs has been associated with a higher methyl ketone content in fulvic acids  
282 fractions as compared to humic acids (Reckhow et al., 1990). In our experiments, no 1,1,1-TCP  
283 could be detected from any isolate. 1,1,1-TCP can be formed by chlorine attack of 1,1-DCP during  
284 chlorination but not during chloramination, because monochloramine is not able to provide further  
285 chlorine substitution (Yang et al., 2007).

### 286 **3.2. Tracing the origin of nitrogen in N-DBPs**

287 To examine the behavior of nitrogen incorporation from organic precursors and  $\text{NH}_2\text{Cl}$ , kinetic  
288 experiments were performed with SR HPOA, JW HPO, JW TPI, JW COL, and RR HPI isolates (5  
289 mg C/L) using  $^{15}\text{N}$ -labeled monochloramine ( $^{15}\text{NH}_2\text{Cl}$ ) (15 mg/L as  $\text{Cl}_2$ ). DBP formation kinetics in  
290 the presence of  $^{15}\text{NH}_2\text{Cl}$  exhibited similar profiles than those obtained using  $^{14}\text{NH}_2\text{Cl}$ . As depicted  
291 on [Fig. S3](#) and [S4](#) (SI) for each DOM isolate, the initial fast reaction occurring before 24h was  
292 generally related to the incorporation of  $^{14}\text{N}$  from N-org precursors into DCACAm and DCAN. This  
293 result is in accordance with the faster reactivity of JW TPI observed in the first 24 hours of reaction

294 (Fig. 1) as compared to JW HPO which can be attributed to its higher nitrogen content (i.e., lower  
 295 C/N ratio). Overall, the isolates exhibited a slow and linear formation of <sup>15</sup>N-DCAcAm and  
 296 <sup>15</sup>N-DCAN, while the formation of <sup>14</sup>N-DCAcAm and <sup>14</sup>N-DCAN tended to reach a plateau during  
 297 the 72-hour reaction time. For SR HPOA, showing very low nitrogen content, the incorporation of  
 298 inorganic nitrogen from NH<sub>2</sub>Cl was the predominant mechanism after 10 hours of reaction (e.g.,  
 299 84.6% of the DCAcAm formed at 48h was <sup>15</sup>N-DCAcAm), which explains the steep linear kinetics  
 300 profiles obtained for DCAN and DCAcAm in the preliminary experiments. JW HPO profiles were  
 301 similar to those of SR HPOA, showing proportions of <sup>15</sup>N-DCAcAm and <sup>15</sup>N-DCAN at 72h of  
 302 74.6% and 68.5%, respectively, which also explains the linearity of profiles shown in Fig. 1. In  
 303 contrast, the formation of N-DBPs from the JW TPI isolate was more influenced by both  
 304 mechanisms at the same time (e.g., the proportion of <sup>15</sup>N-DCAcAm was 49% ± 10% throughout the  
 305 reaction time) thus explaining the non-linear profiles obtained. In the case of the RR HPI isolate, the  
 306 formation of <sup>15</sup>N-DCAcAm was slower than that of <sup>14</sup>N-DCAcAm in the first 40 hours of reaction  
 307 but finally reached a similar concentration after 48h (i.e., 20.3 nM and 18.3 nM, respectively).  
 308 A recent study demonstrated that formation kinetics of N-DBPs (DCAN and TCNM) during  
 309 chloramination are influenced by two contributions: second-order reaction kinetics from N-org  
 310 precursors and the incorporation of inorganic nitrogen from chloramines, linearly correlated with  
 311 chloramines exposure (Chuang and Tung, 2015). Second-order reaction kinetics for <sup>14</sup>N-DBP  
 312 depends on the concentrations of NH<sub>2</sub>Cl and <sup>14</sup>N-DBP precursors, and can be expressed as Eq. 1:



$$\frac{d[^{14}\text{NDBP}]}{dt} = k [^{14}\text{NDBP precursors}][\text{NH}_2\text{Cl}],$$

313 Where k is the second-order rate constant for the formation of <sup>14</sup>N-DBPs. Integrating Eq. 1 for t  
 314 yields Eq. 2 (Text S2, SI).

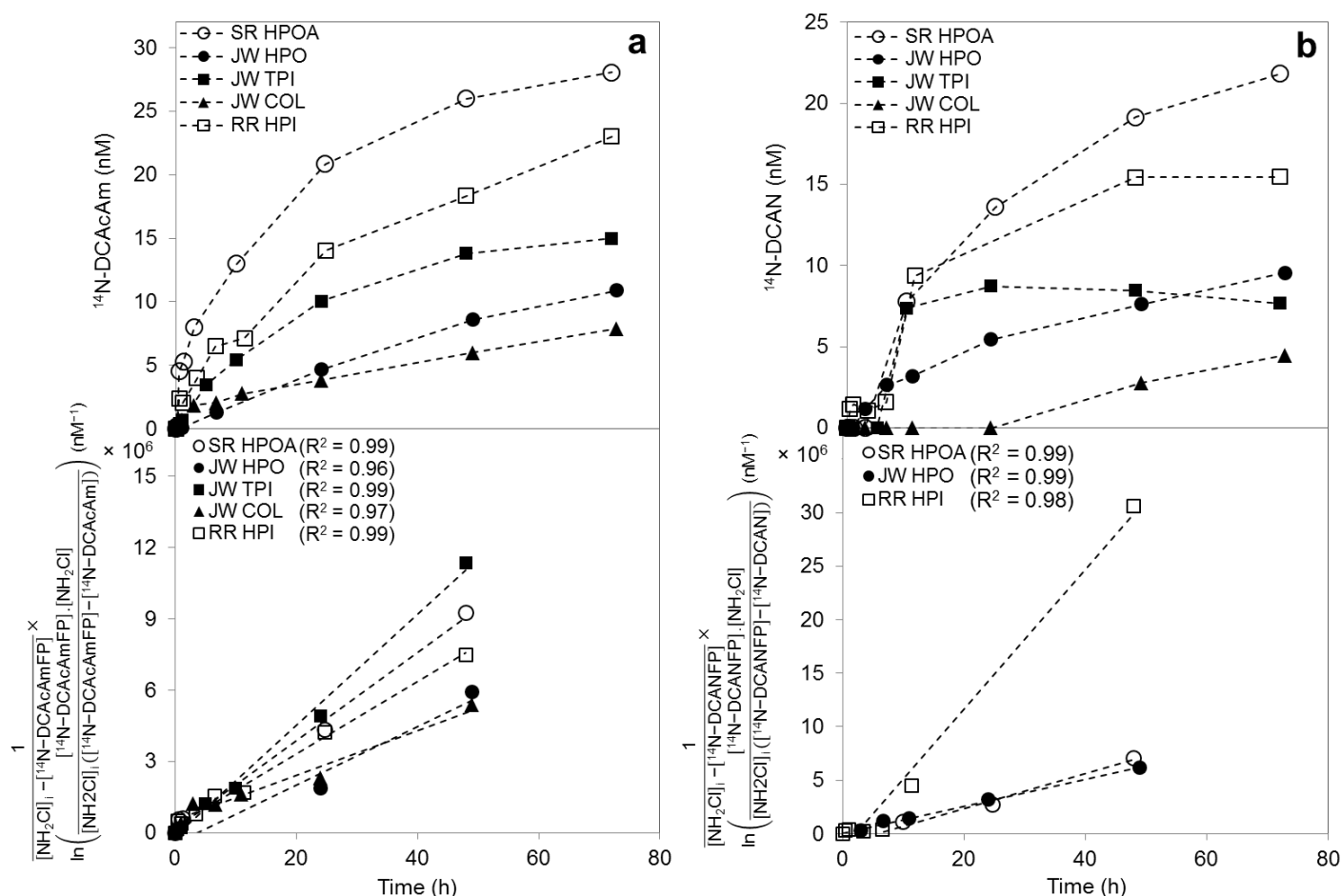
$$\frac{1}{([\text{NH}_2\text{Cl}]_i - [^{14}\text{NDBP precursors}]_{\text{total}})}$$

$$\times \ln \left( \frac{[^{14}\text{NDBP precursors}]_{\text{Total}} \times [\text{NH}_2\text{Cl}]}{[\text{NH}_2\text{Cl}]_i \times ([^{14}\text{NDBP precursors}]_{\text{Total}} - [^{14}\text{NDBP}])} \right) = kt \quad (2)$$

315

316 where  $[\text{NH}_2\text{Cl}]_i$  is the initial monochloramine concentration and  $[^{14}\text{N-DBP precursors}]_{\text{Total}}$  is the  
 317 total  $^{14}\text{N-DBP}$  precursors concentration, i.e., the concentration of  $^{14}\text{N-DBP}$  formed at 72h.

318 **Fig. 2** shows the formation of  $^{14}\text{N-DCAcAm}$  and  $^{14}\text{N-DCAN}$  and their respective second-order  
 319 relationships derived from **Eq. 2**. Linear relationships were obtained from this second-order model  
 320 for the formation of the two  $^{14}\text{N-DBPs}$  with most of the investigated isolates. The linearity observed  
 321 for the first 48 hours suggests that the reaction was nearly completed after 72h. This finding  
 322 confirms that  $^{14}\text{N-DBPs}$  produced after 72h can be used to reflect the total concentration of  $^{14}\text{N-}$   
 323  $\text{DBP}$  precursors.  $^{14}\text{N-DCAcAm}$  formation followed second-order kinetics for all the isolates.  
 324 Because JW TPI exhibited a decreasing profile after 24h and not enough data points were obtained  
 325 for JW COL, second-order relationships could not be plotted for  $^{14}\text{N-DCAN}$  formation from these  
 326 two isolates. The SR HPOA isolate exhibited the highest formation of  $^{14}\text{N-DCAcAm}$  (i.e., 28.0  
 327 nM), followed by RR HPI, JW TPI, JW HPO, and finally JW COL. A similar order was obtained for  
 328 the formation of  $^{14}\text{N-DCAN}$ , however, JW TPI showed a slight decrease in concentration after 24h  
 329 of reaction time, reaching a lower value than JW HPO at 72h. Because SR HPOA is characterized  
 330 by the highest C/N ratio (i.e., lowest nitrogenous moieties content) of the studied isolates, these  
 331 results indicate that there is no direct correlation between nitrogen content of DOM and the  
 332 production of  $^{14}\text{N-DCAcAm}$  or  $^{14}\text{N-DCAN}$ . Hence, the reactivity of specific organic nitrogen sites  
 333 plays a more important role in SR HPOA as compared to other fractions of DOM. The aromatic  
 334 character does not seem to be a critical parameter in the formation of  $^{14}\text{N-DBPs}$ , since low SUVA  
 335 isolates (e.g., RR HPI) exhibited higher formation of  $^{14}\text{N-DCAcAm}$  and  $^{14}\text{N-DCAN}$  than higher  
 336 SUVA isolates (e.g., JW HPO).



337

Figure 2. Formation of a)  $^{14}\text{N}$ -DCAcAm and b)  $^{14}\text{N}$ -DCAN and their respective second-order relationships for SR HPOA, RR HPI, JW HPO, JW TPI, and JW COL isolates (5 mg C/L) and  $^{15}\text{NH}_2\text{Cl}$  (15 mg  $\text{Cl}_2/\text{L}$ ) at pH 8 (10 mM phosphate buffer) over 72h.

338

As proposed in the literature (Chuang and Tung, 2015), a linear correlation was observed between

339

$^{15}\text{N}$ -DCAN formation and monochloramine exposure for all isolates investigated (Fig. 3). The same

340

linear correlation was observed for the formation of  $^{15}\text{N}$ -DCAcAm. SR HPOA exhibited again the

341

highest reactivity, with concentrations of up to 143.2 nM of  $^{15}\text{N}$ -DCAcAm and 73.4 nM of  $^{15}\text{N}$ -

342

DCAN formed after 48h (i.e., an exposure of 33,922 mg.min/L). In general, isolates with higher

343

SUVA values exhibited more pronounced slopes, which indicates that a major incorporation of  $^{15}\text{N}$

344

occurs during  $^{15}\text{NH}_2\text{Cl}$  reaction with organic matter enriched in aromatic moieties. RR HPI formed

345

the highest proportion of  $^{14}\text{N}$ -DCAcAm (i.e., 47.4% at 48h) as compared to  $^{15}\text{N}$ -DCAcAm. The

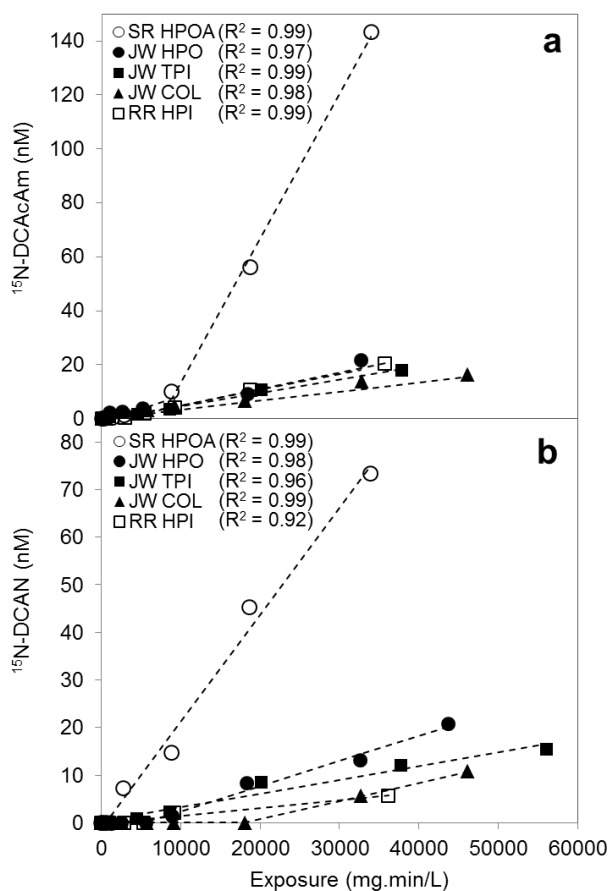
346

comparison was even more significant for DCAN, with a relative abundance of 72.1% of

347

$^{14}\text{N}$ -DCAN at 48h, indicating that hydrophilic fractions of DOM enriched in nitrogen (see C/N

348 ratios in Table S2, SI) incorporate a higher proportion of nitrogen from N-org precursors into  
349 N-DBPs.



350

Figure 3. Formation of a)  $^{15}\text{N}$ -DCAcAm and b)  $^{15}\text{N}$ -DCAN from SR HPOA, RR HPI, JW HPO, JW TPI, and JW COL isolates (5 mg C/L) and  $^{15}\text{NH}_2\text{Cl}$  (15 mg  $\text{Cl}_2/\text{L}$ ) at pH 8 (10 mM phosphate buffer) over 72h.

351 These results explain the N-DBP formation profiles obtained in the experiments involving only  
352  $^{14}\text{NH}_2\text{Cl}$  (Fig. 1). The first step of rapid N-DBP production is related to the reactivity of N-org  
353 precursors with chlorine atoms of  $\text{NH}_2\text{Cl}$ . As N-org precursors (i.e.,  $^{14}\text{N}$ -DBP precursors) are  
354 consumed, the formation of  $^{14}\text{N}$ -DBP tends to stabilize as described by the second-order reaction  
355 kinetics. Then, the contribution of non-nitrogenous precursors starts to be significant, exhibiting a  
356 slower reactivity with  $\text{NH}_2\text{Cl}$  but finally reaching high N-DBP concentrations. These high  
357 concentrations may be due to the higher initial concentrations of non-nitrogenous precursors, i.e.,  
358 aromatic precursors, as compared to N-org precursors. The second step of linear increase with  
359 increasing exposure can thus be described as the slow incorporation of nitrogen from  $\text{NH}_2\text{Cl}$  into

360 non-nitrogenous precursors comprising aromatic moieties.

361 Aldehydes are known to be precursors of nitriles, and it has been demonstrated that

362 chloroacetaldehyde forms chloroacetamide and N,2-dichloroacetamide (first time identified) in

363 alkaline chloramination conditions (Kimura et al., 2013). HAcAms can thus be expected to be

364 formed from haloacetaldehydes (HAcAl) either directly through the Aldehyde Pathway or indirectly

365 through the hydrolysis of HANs. DCaAcAl and TCaAcAl were monitored during the kinetics studies

366 involving  $^{15}\text{N-NH}_2\text{Cl}$  to compare their formation with HAcAms formation (Fig. 4). TCaAcAl was

367 only detected with JW HPO at very low concentrations (7.7 nM at 72h). DCaAcAl formation did not

368 fit with any second-order kinetics and a linear correlation with oxidant exposure could not be

369 established. As described in Fig. 4b for JW HPO, the kinetics of formation followed a 2<sup>nd</sup> order-like

370 profile in the first 10 hours of reaction and then linearly increased with monochloramine exposure,

371 reaching a concentration of 28.5 nM after 72h. Similarly to N-DBPs, DCaAcAl formation could be

372 attributed to two types of reaction mechanisms: a) a formation from N-org precursors or an

373 intermediate in the first hours of reaction, followed by b) a slow reaction with monochloramine.

374 This second step of formation could be linked to the formation of DCaAcAm, i.e., the linear increase

375 in DCaAcAm concentrations would follow the linear formation of DCaAcAl through the

376 incorporation of a N atom from  $\text{NH}_2\text{Cl}$  and the formation of a carbinolamine

377 (2-dichloro-1-(chloroamino)ethanol) and a *N*-chloroamide (*N*-chlorodichloroacetamide)

378 intermediate (Kimura et al., 2013). The formation of *N*-chlorodichloroacetamide has been reported

379 during chlorination of DCAN at pH 10 (Peters et al., 1990). It was not detected at lower pH values,

380 because *N*-chloroamides are easily hydrolyzed in the presence of HOCl. Samples from this study

381 were analyzed in full scan mode GC-MS, but no peaks corresponded to the abovementioned

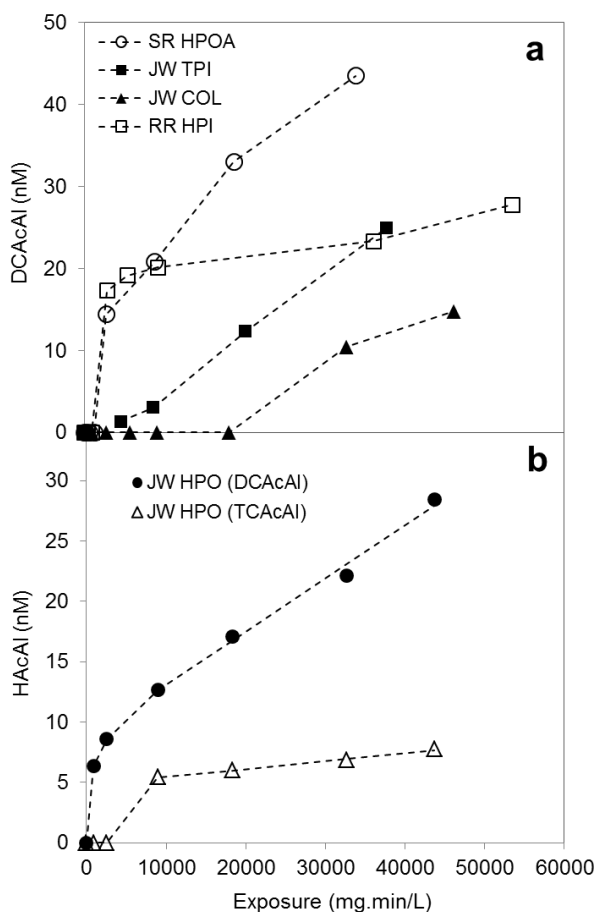
382 intermediates. Despite its two-steps profile, DCaAcAl formation from JW HPO did not exhibit the

383 same kinetics profile as DCaAcAm and DCAN formation, since more DCaAcAl was formed in the

384 first hours of reaction and the linear increase of DCaAcAm and DCAN was finally more pronounced

385 than that of DCaAcAl (Fig. S6, SI). A similar observation was made from SR HPOA, which formed

386 the highest DCaAcAl concentration (43.5 nM at 72h) but in limited proportions as compared to  
 387 DCaAcAm and DCAN. These results indicate that DCaAcAl formation followed an independent  
 388 pathway from DCaAcAm formation. However, additional investigations are needed to confirm this  
 389 hypothesis.  
 390



391  
 Figure 4. Formation of a) DCaAcAl and b) DCaAcAl and TCaAcAl from SR HPOA, RR HPI, JW HPO, JW TPI, and JW COL isolates (5 mg C/L) and  $^{15}\text{NH}_2\text{Cl}$  (15 mg  $\text{Cl}_2/\text{L}$ ) at pH 8 (10 mM phosphate buffer) over 72h.

In contrast to other DBPs, the production of DCAA from SR HPOA exhibited the exact same formation profile as total DCaAcAm (i.e., the sum of  $^{14}\text{N}$ -DCaAcAm and  $^{15}\text{N}$ -DCaAcAm), and their concentrations were strongly correlated along the reaction time ( $R^2 = 0.999$ ) (Fig. S7, SI). Good fittings were also obtained for other DOM isolates ( $R^2$  ranging from 0.96 to 0.98). DCAA concentrations were approximately two times higher than DCaAcAm concentrations for all isolates

(i.e., the average slope was  $2.1 \pm 0.5$ ). This result indicates a direct relationship between the two DBPs during chloramination of DOM, which can be related to the hydrolysis of DCACAm to DCAA observed during chlorination (Peters et al., 1990; Reckhow et al., 2001).

392 While the formation of 1,1-DCP mainly occurred from DOM isolates presenting a strong aromatic  
393 character (Table S3, SI), its formation did not linearly increase with chloramine exposure and  
394 followed second-order kinetics (Fig. S5, SI). This different behavior compared to those of DCAN  
395 and DCACAm indicates that its formation mechanism follows a more complex pathway than the  
396 solely incorporation of  $^{15}\text{NH}_2\text{Cl}$  in aromatic moieties. Since 1,1-DCP kinetics reached a plateau at  
397 reaction times where DCAN and DCACAm were still linearly increasing, its formation might  
398 depend on the availability of an intermediate rather than that of aromatic precursors.

### 399 **3.3. DBP Formation Potentials**

400 To verify the hypothesis of the aromatic character of DOM playing a role in the formation of  
401 N-DBPs during chloramination, DBP formation potentials from seven DOM isolates were  
402 determined after 72h of chloramination using  $^{15}\text{NH}_2\text{Cl}$  at pH 8. As previously observed, major DBP  
403 species produced for each class of monitored DBPs (i.e., HAAs, HAcAms, HAcAls) were  
404 dichlorinated in the experimental conditions used. Similarly to the kinetics experiments, DCAA was  
405 the major DBP analyzed for all the isolates, with concentrations ranging between 56.0 nM (JW  
406 COL) and 594.6 nM (BR HPO). DCAA concentrations were higher than TCM concentrations, in  
407 accordance with previous studies conducted on the chloramination of natural waters (Hua and  
408 Reckhow, 2007). DCACAm exhibited the highest concentrations after DCAA and TCM, reaching  
409 132 ( $\pm 76$ ) nM for SR HPOA. DCACAl concentrations were close to those of DCAN, ranging from  
410 14.8 nM (JW COL) to 40.4 nM (SR HPOA). TCAA and TCACAl were also observed at low  
411 concentrations (4.0 to 7.7 nM) (Table S3, SI).

412 Almost all isolates exhibited a higher proportion of  $^{15}\text{N}$  incorporation than  $^{14}\text{N}$ , either in  
413 DCACAm or in DCAN (i.e., only RR HPI formed more  $^{14}\text{N}$ -DCAN than  $^{15}\text{N}$ -DCAN) (Table 1).  
414 Similarly to results obtained from kinetics experiments, the highest concentrations of either

415  $^{14}\text{N}$ -DBPs or  $^{15}\text{N}$ -DBPs were obtained with SR HPOA. Even if no correlation could be derived  
416 from the whole set of results, the general trend was the higher the SUVA of the DOM isolate the  
417 higher the incorporation of  $^{15}\text{N}$  in N-DBPs (Fig. S8, SI). When discriminating the OM isolates as a  
418 function of their origin (i.e., 3 HPO fractions from river waters in one group and 3 fractions from  
419 wastewater effluent in another group), good correlations were obtained between  $^{15}\text{N}$ -DBPs  
420 formation and SUVA values ( $R^2 = 0.92$  for  $^{15}\text{N}$ -DCAcAm and  $R^2 = 0.999$  for  $^{15}\text{N}$ -DCAN) (Fig. S8  
421 and Table S4, SI). These results are in good agreement with previous studies which demonstrated  
422 that the formation of DCAN during chloramination did not correlate with DON/DOC ratio values of  
423 DOM fractions but correlated well with their SUVA values (Yang et al., 2008). In addition to these  
424 correlations with SUVA,  $^{15}\text{N}$ -DCAcAm and  $^{15}\text{N}$ -DCAN formations exhibited a linear relationship  
425 against each other ( $R^2 = 0.93$ , Fig. 5). This observation suggests a similar behavior of DCAcAm and  
426 DCAN towards the incorporation of  $^{15}\text{NH}_2\text{Cl}$  as SUVA of DOM increases. Such a relationship  
427 could not be established from  $^{14}\text{N}$ -DCAcAm and  $^{14}\text{N}$ -DCAN, suggesting that  $^{14}\text{N}$  incorporation did  
428 not follow a common pattern for the two species of DBPs. This agrees with results from Huang et  
429 al. (2012), who proposed that DCAcAm formation could be independent from DCAN hydrolysis.  
430 DCAcAm formation from humic-like materials was proposed to rapidly occur through the  
431 Decarboxylation Pathway, followed by the incorporation of inorganic nitrogen through the  
432 Aldehyde Pathway becoming more important with increasing chloramines exposure. Thus, DCAN  
433 and DCAcAm formation would follow similar but independent pathways during the chloramination  
434 of humic substances.

435

436 Table 1. Proportion of nitrogen incorporation in DCAN and DCAcAm by chloramination (15 mg  
437  $\text{Cl}_2/\text{L}$ ) of OM isolates (DOC = 5 mg C/L) at pH 8 during 72h of contact time.

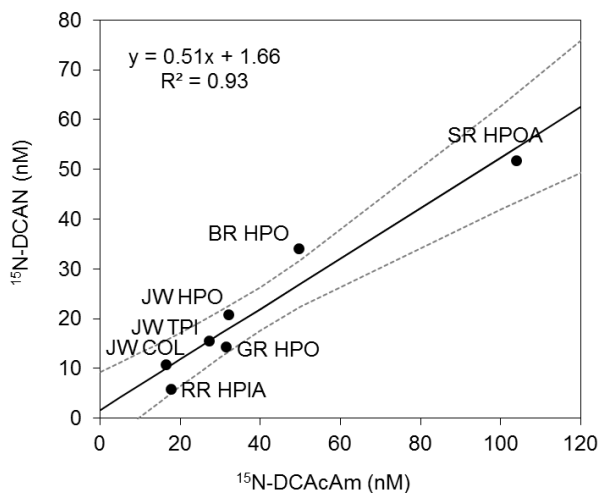
Isolate	Concentration (nM) (N incorporation - % <sup>a</sup> )			
	$^{14}\text{N}$ -DCAN	$^{15}\text{N}$ -DCAN	$^{14}\text{N}$ -DCAcAm	$^{15}\text{N}$ -DCAcAm
SR HPOA	19.1 (27)	51.8 (73)	28.0 (21)	104.0 (79)

BR HPO	8.7 (20)	34.1 (80)	13.7 (22)	49.7 (78)
GR HPO	2.0 (12)	14.3 (88)	11.2 (26)	31.5 (74)
RR HPI	11.3 (66)	5.8 (34)	13.9 (44)	17.7 (56)
JW HPO	10.9 (34)	20.7 (66)	2.0 (33)	4.1 (67)
JW TPI	7.7 (33)	15.4 (67)	3.0 (46)	3.5 (54)
JW COL	4.5 (29)	10.8 (71)	11.4 (41)	16.5 (59)

<sup>a</sup> N incorporation = nitrogen proportion in N-DBPs, calculated as

$$\frac{[^{14}\text{or}^{15}\text{NDBP}] \times 100}{([^{14}\text{NDBP}] + [^{15}\text{NDBP}])} (\%)$$

438



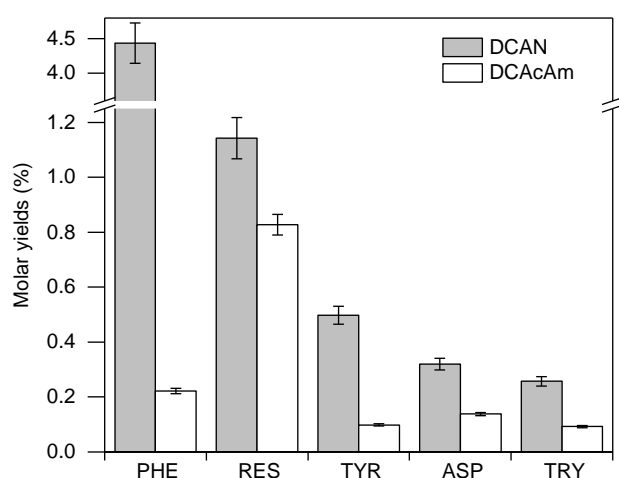
439

Figure 5. Relationship between <sup>15</sup>N-DCAN and <sup>15</sup>N-DCAcAm formation potentials after chloramination (<sup>15</sup>NH<sub>2</sub>Cl = 15 mg Cl<sub>2</sub>/L) of DOM isolates (DOC = 5 mg C/L) at pH 8 (10 mM phosphate buffer) during 72h. Dashed lines represent 95% interval confidence.

#### 440 3.4. N-DBP formation potentials from model compounds

441 Most studies using model precursors for HANs and HAcAms formation during chlorination and  
 442 chloramination have focused on amino acids (e.g., asparagine, aspartic acid) (Chu et al., 2012; Chu  
 443 et al., 2010b; Huang et al., 2012; Trehy et al., 1986; Yang et al., 2010, 2012). Aromatic amino acids  
 444 (i.e., tryptophan and tyrosine) were demonstrated as important precursors of HAcAms. A  
 445 mechanism was recently proposed to describe the formation of TCAC from the aromatic ring of  
 446 tyrosine (Chu et al., 2012). Multiple chlorine attacks on the phenolic ring form chloro-, dichloro-  
 447 and trichloro-phenol, ring opening released chloroform, TCAA and a trichloroacetyl chloride  
 448 (TCAC) intermediate (tentative structure identified by GC-MS). The last step would form TCACAm  
 449 through TCAC reaction with ammonia and the elimination of hydrochloric acid. However, the  
 450 mechanism of this critical step, leading to the formation of the amide group (i.e., nitrogen

451 incorporation), is still uncertain. Such a pathway was not described for DCaAm, which was  
452 thought to be formed only from DCAN hydrolysis (Chu et al., 2012). However, DCaAm was  
453 suggested to be formed independently from DCAN hydrolysis during the chloramination of humic  
454 substances (Huang et al., 2012). To investigate the reactivity of aromatic compounds with  
455 monochloramine, N-DBPs formation tests were conducted by chloramination (100 mg Cl<sub>2</sub>/L) of  
456 250 μM phenol (PHE) and resorcinol (RES) for 72h at pH 7, and results were compared with amino  
457 acids previously described as major precursors of N-DBPs (e.g., tyrosine - TYR, aspartic acid -  
458 ASP, tryptophan - TRY) (Fig. 6). Phenol and resorcinol formed higher concentrations of DCAN and  
459 DCaAm than the amino acids, proving that aromatic compounds can be major precursors of  
460 N-DBPs as compared to other previously proposed nitrogenous precursors. Phenol produced the  
461 highest yield of DCAN (4.43% molar yield), while the highest proportion of DCaAm was  
462 obtained from resorcinol (0.83%). This result can be related to the presence of the second hydroxyl  
463 group in meta position, known to activate the aromatic ring for electrophilic substitution by  
464 chlorine. While the incorporation of nitrogen from NH<sub>2</sub>Cl was previously hypothesized to occur  
465 through the Aldehyde Pathway (Huang et al., 2012), these results show that aromatic organic  
466 compounds react with monochloramine to produce N-DBPs through an unknown mechanism.  
467



468  
469 Figure 6. DCAN and DCaAm formation by chloramination (100 mg Cl<sub>2</sub>/L) of phenol, resorcinol,  
470 tyrosine, aspartic acid, and tryptophan (250 μM) over 72 h and at pH 7 (10 mM phosphate buffer).

471 Molar yields were calculated based upon the initial model precursor concentration. Error bars  
472 represent standard deviations (n = 3). PHE: phenol; RES: resorcinol; TYR: tyrosine; ASP: aspartic  
473 acid; TRY: tryptophan.

474

#### 475 **4. Conclusions**

476 This study demonstrates the possibility of N-DBPs formation from aromatic moieties of DOM.  
477 Experiments using aromatic model compounds confirm the results obtained from DOM isolates.  
478 The results from this investigation are of significant importance for water treatment facilities using  
479 chloramines as final disinfectant, where the removal of aromatic DOC must be optimized to avoid  
480 the production of N-DBPs. This work also confirms the possibility of two distinct mechanisms  
481 explaining N-DBP formation during chlorination/chloramination of aromatic amino acids, i.e.,  
482 chlorination of amino groups and incorporation of inorganic nitrogen from  $\text{NH}_2\text{Cl}$  in aromatic rings.  
483 The mechanism of N-DBPs formation through aromatic ring opening and nitrogen incorporation  
484 requires further investigation to be elucidated. Kinetics experiments and structural identifications of  
485 potential reaction intermediates should be performed in order to understand this pathway. Potential  
486 intermediates include carbinolamines and N-chloroamides, both previously observed as  
487 intermediates during the chloramination of aldehydes and the chlorination of acetamides,  
488 respectively.

489

#### 490 **Acknowledgments**

491 Research reported in this publication was supported by the King Abdullah University of Science  
492 and Technology (KAUST). The authors would also like to thank Dr. Leo Gutierrez for his  
493 assistance and support.

494

#### 495 **Appendix. Supplementary Material.**

496 Supplementary information file includes analytical details, characteristics of DOM isolates, raw  
497 DBP results tables and additional figures.

498

## 499 **References**

500 Bond, T., Henriot, O., Goslan, E.H., Parsons, S.A., Jefferson, B., 2009. Disinfection byproduct  
501 formation and fractionation behavior of natural organic matter surrogates. *Environmental Science*  
502 *and Technology* 43, 5982–5989.

503 Bond, T., Huang, J., Templeton, M.R., Graham, N., 2011. Occurrence and control of nitrogenous  
504 disinfection by-products in drinking water – A review. *Water Research* 45, 4341–4354.

505 Bond, T., Templeton, M.R., Graham, N., 2012. Precursors of nitrogenous disinfection by-products  
506 in drinking water—A critical review and analysis. *Journal of Hazardous Materials* 235–236, 1–16.

507 Chuang, Y.-H., Lin, A.Y.-C., Wang, X., Tung, H., 2013. The contribution of dissolved organic  
508 nitrogen and chloramines to nitrogenous disinfection byproduct formation from natural organic  
509 matter. *Water Research* 47, 1308–1316.

510 Chuang, Y.-H., Tung, H., 2015. Formation of trichloronitromethane and dichloroacetonitrile in  
511 natural waters: Precursor characterization, kinetics and interpretation. *Journal of Hazardous*  
512 *Materials* 283, 218–226.

513 Chu, W., Gao, N., Deng, Y., 2010a. Formation of haloacetamides during chlorination of dissolved  
514 organic nitrogen aspartic acid. *Journal of Hazardous Materials* 173, 82–86.

515 Chu, W., Gao, N., Krasner, S.W., Templeton, M.R., Yin, D., 2012. Formation of halogenated C-, N-  
516 DBPs from chlor(am)ination and UV irradiation of tyrosine in drinking water. *Environmental*  
517 *Pollution* 161, 8–14.

518 Chu, W., Gao, N.-Y., Deng, Y., Krasner, S.W., 2010b. Precursors of dichloroacetamide, an emerging  
519 nitrogenous DBP formed during chlorination or chloramination. *Environmental Science and*  
520 *Technology* 44, 3908–3912.

521 Chu, W., Gao, N., Yin, D., Krasner, S.W., 2013. Formation and speciation of nine haloacetamides,  
522 an emerging class of nitrogenous DBPs, during chlorination or chloramination. *Journal of*  
523 *Hazardous Materials* 260, 806–812.

524 Croué, J.-P., 2004. Isolation of Humic and Non-Humic NOM Fractions: Structural Characterization.  
525 *Environmental Monitoring and Assessment* 92, 193–207.

526 Dotson, A., Westerhoff, P., Krasner, S.W., 2009. Nitrogen enriched dissolved organic matter (DOM)

527 isolates and their affinity to form emerging disinfection by-products. *Water Science and Technology*  
528 60, 135–143.

529 Drewes, J.E., Croue, J.-P., 2002. New approaches for structural characterization of organic matter in  
530 drinking water and wastewater effluents, *Water Science and Technology: Water Supply* 2, 1-10.

531 Eaton, A.D., Clesceri, L.S., Greenberg, A.E., Eds. *Standard Methods for the Examination of Water*  
532 *and Wastewater*, 19th ed.; American Public Health Association/American Water Works  
533 Association/Water Environment Federation Publishers; Washington D.C., USA, 1995.

534 Fang, J., Ma, J., Yang, X., Shang, C., 2010. Formation of carbonaceous and nitrogenous disinfection  
535 by-products from the chlorination of *Microcystis aeruginosa*. *Water Research* 44, 1934–1940.

536 Glezer, V., Harris, B., Tal, N., Iosefzon, B., Lev, O., 1999. Hydrolysis of haloacetonitriles: Linear  
537 free energy relationship. Kinetics and products. *Water Research* 33, 1938–1948.

538 Gonsior, M., Zwartjes, M., Cooper, W.J., Song, W., Ishida, K.P., Tseng, L.Y., Jeung, M.K., Rosso,  
539 D., Hertkorn, N., Schmitt-Kopplin, P., 2011. Molecular characterization of effluent organic matter  
540 identified by ultrahigh resolution mass spectrometry. *Water Research* 45, 2943 – 2953.

541 Hua, G., Reckhow, D.A., 2007. Comparison of disinfection byproduct formation from chlorine and  
542 alternative disinfectants. *Water Research* 41, 1667–1678.

543 Huang, H., Wu, Q.-Y., Hu, H.-Y., Mitch, W.A., 2012. Dichloroacetonitrile and dichloroacetamide  
544 can form independently during chlorination and chloramination of drinking waters, model organic  
545 matters, and wastewater effluents. *Environmental Science and Technology* 46, 10624–10631.

546 Huang, H., Wu, Q.-Y., Tang, X., Jiang, R., Hu, H.-Y., 2013. Formation of haloacetonitriles and  
547 haloacetamides during chlorination of pure culture bacteria. *Chemosphere* 92, 375–381.

548 Jafvert, C.T., Valentine, R.L., 1992. Reaction scheme for the chlorination of ammoniacal water.  
549 *Environmental Science and Technology* 26, 577–786.

550 Kimura, S.Y., Komaki, Y., Plewa, M.J., Mariñas, B.J., 2013. Chloroacetonitrile and N,2-  
551 dichloroacetamide formation from the reaction of chloroacetaldehyde and monochloramine in  
552 water. *Environmental Science and Technology* 47, 12382–12390.

553 Krasner, S.W., Scilimenti, M.J., Mitch, W., Westerhoff, P., Dotson, A., 2007. Using formation  
554 potential tests to elucidate the reactivity of DBP precursors with chlorine versus with chloramines,  
555 in: *Proceedings of the 2007 AWWA Water Quality Technology Conference*, Denver. AWWA.

556 Krasner, S.W., Weinberg, H.S., Richardson, S.D., Pastor, S.J., Chinn, R., Scilimenti, M.J., Onstad,  
557 G.D., Thruston Jr, A.D., 2006. Occurrence of a new generation of disinfection byproducts.

558 Environmental Science and Technology 40, 7175–7185.

559 Leenheer, J.A., Croué, J.P., 2003. Characterizing aquatic dissolved organic matter. Environmental  
560 Science and Technology 37, 18A–26A.

561 Leenheer, J.A., Croué, J.P., Benjamin, M., Korshin, G.V., Hwang, C.J., Bruchet, A., Aiken, G.R.,  
562 2000. Comprehensive Isolation of Natural Organic Matter from Water for Spectral  
563 Characterizations and Reactivity Testing, in: *Natural Organic Matter and Disinfection By-Products*,  
564 *ACS Symposium Series*. American Chemical Society, pp. 68–83.

565 Mitch, W.A., Sedlak, D.L., 2004. Characterization and Fate of N-Nitrosodimethylamine Precursors  
566 in Municipal Wastewater Treatment Plants. Environmental Science and Technology 38, 1445–1454.

567 Muellner, M.G., Wagner, E.D., Mccalla, K., Richardson, S.D., Woo, Y.-T., Plewa, M.J., 2007.  
568 Haloacetonitriles vs. regulated haloacetic acids: Are nitrogen-containing DBPs more toxic?  
569 Environmental Science and Technology 41, 645–651.

570 Munch, D.J., Hautman, D.P., 1995. EPA Method 551.1 Determination of Chlorination Disinfection  
571 Byproducts, Chlorinated Solvents, and Halogenated Pesticides/Herbicides in Drinking Water by  
572 Liquid-Liquid Extraction and Gas Chromatography with Electron-Capture Detection, Revision 1.0.  
573 United States Environmental Protection Agency, Cincinnati, OH.

574 Munch, D.J., Munch, J.W., 1995. EPA Method 552.2 Determination of Haloacetic Acids and  
575 Dalapon in Drinking Water by Liquid-liquid Extraction, Derivatization and Gas Chromatography  
576 with Electron Capture Detection, Revision 1.0. United States Environmental Protection Agency,  
577 Cincinnati, OH.

578 Oliver, B.G., 1983. Dihaloacetonitriles in drinking water: Algae and fulvic acid as precursors.  
579 Environmental Science and Technology 17, 80–83.

580 Pedersen, E.J., Urbansky, E.T., Marinas, B.J., Margerum, D.W., 1999. Formation of Cyanogen  
581 Chloride from the Reaction of Monochloramine with Formaldehyde. Environmental Science and  
582 Technology 33, 4239–4249.

583 Peters, R.J.B., De Leer, W.B.E., De Galan, L., 1990. Chlorination of cyanoethanoic acid in aqueous  
584 medium. Environmental Science and Technology 24, 81–86.

585 Plewa, M.J., Wagner, E.D., Jazwierska, P., Richardson, S.D., Chen, P.H., McKague, A.B., 2004.  
586 Halonitromethane drinking water disinfection byproducts: Chemical characterization and  
587 mammalian cell cytotoxicity and genotoxicity. Environmental Science and Technology 38, 62–68.

588 Plewa, M.J., Wagner, E.D., Muellner, M.G., Hsu, K.-M., Richardson, S.D., 2008. Comparative  
589 Mammalian Cell Toxicity of N-DBPs and C-DBPs, in: *Disinfection By-Products in Drinking Water*,

590 *ACS Symposium Series*. American Chemical Society, pp. 36–50.

591 Reckhow, D.A., MacNeill, A.L., Platt, T.L., MacNeill, A.L., McClellan, J.N., 2001. Formation and  
592 degradation of dichloroacetonitrile in drinking waters. *Journal of Water Supply: Research and*  
593 *Technology - AQUA* 50, 1–13.

594 Reckhow, D.A., Singer, P.C., 1985. Mechanisms of organic halide formation during fulvic acid  
595 chlorination and implications with respect to preozonation, in: *Water Chlorination Chemistry:*  
596 *Environmental Impact and Health Effects*. Jolley R.L. Ann Arbor Science Publishers, p. 1229.

597 Reckhow, D.A., Singer, P.C., Malcolm, R.L., 1990. Chlorination of humic materials: Byproduct  
598 formation and chemical interpretations. *Environmental Science and Technology* 24, 1655–1664.

599 Schreiber, I.M., Mitch, W.A., 2005. Influence of the order of reagent addition on NDMA formation  
600 during chloramination. *Environmental Science and Technology* 39, 3811–3818.

601 Suffet, I.H., Brenner, L., Silver, B., 1976. Identification of 1,1,1-trichloroacetone (1,1,1-  
602 trichloropropanone) in two drinking waters: a known precursor in haloform reaction. *Environmental*  
603 *Science and Technology* 10, 1273–1275.

604 Trehay, M.L., Yost, R.A., Miles, C.J., 1986. Chlorination byproducts of amino acids in natural  
605 waters. *Environmental Science and Technology* 20, 1117–1122.

606 Weinberg, H.S., Krasner, S.W., Richardson, S.D., Thruston Jr, A.D., 2002. The Occurrence of  
607 Disinfection By-Products (DBPs) of Health Concern in Drinking Water: Results of a Nationwide  
608 DBP Occurrence Study; EPA/600/R02/068.

609 Westerhoff, P., Mash, H., 2002. Dissolved organic nitrogen in drinking water supplies: A review.  
610 *Journal of Water Supply: Research and Technology - AQUA* 51, 415–448.

611 Yang, X., Fan, C., Shang, C., Zhao, Q., 2010. Nitrogenous disinfection byproducts formation and  
612 nitrogen origin exploration during chloramination of nitrogenous organic compounds. *Water*  
613 *Research* 44, 2691–2702.

614 Yang, X., Guo, W., Shen, Q., 2011. Formation of disinfection byproducts from chlor(am)ination of  
615 algal organic matter. *Journal of Hazardous Materials* 197, 378–388.

616 Yang, X., Shang, C., Lee, W., Westerhoff, P., Fan, C., 2008. Correlations between organic matter  
617 properties and DBP formation during chloramination. *Water Research* 42, 2329–2339.

618 Yang, X., Shang, C., Westerhoff, P., 2007. Factors affecting formation of haloacetonitriles,  
619 halo ketones, chloropicrin and cyanogen halides during chloramination. *Water Research* 41, 1193–  
620 1200.

621 Yang, X., Shen, Q., Guo, W., Peng, J., Liang, Y., 2012. Precursors and nitrogen origins of  
622 trichloronitromethane and dichloroacetonitrile during chlorination/chloramination. *Chemosphere*  
623 88, 25–32.  
624